UV irradiation of PVA-3%M, (M=NiO, MgO, Al_2O_3) nanoparticles for medical applications

M. Rashad[a,b*], A. Al-Qarni[a], J. Al-Muayqili[a], I. Al-Qarni[a], J. Al-Rashidi[a], F. A. Al-Shehri[a], S. Al-Ghamdi[a], M. M. Al-Balawi[a], S. A. Al-Ghamdi[a], T. A. Hanafy[a,c], F. Al-Rubaie[a]

[a]*Physics Department, Faculty of Science, University of Tabuk, Tabuk 71491, Saudi Arabia*

[b]*Physics Department, Faculty of Science, Assiut University, Assiut 71516, Egypt*

[c]*Department of Physics, Faculty of Science, Fayoum University, El Fayoum, 63514, Egypt*

Polyvinyl Alcohol (PVA) of PVA-3%M, where M stands for NiO, MgO, and Al_2O_3, has been created. Characterization was done using X-ray diffraction (XRD). This characteristic verified the production of the generated oxide NPs during chemical precipitation in PVA. The PVA-3% M nanoparticles (M=NiO, MgO, and Al_2O_3) were examined for their optical characteristics. After 60 minutes, the PVA-3% M nanoparticles (M=NiO, MgO, and Al_2O_3) were subjected to UV light irradiation to examine its effects. The optical properties have been studied in UVA (315–400 nm) area, or long-wave UV, in energy of (3.9–3.1) eV. Time under UV light has an impact on the optical energy gap of PVA-3% M. As a function of the UV exposure time, the optical characteristics of PVA-3% M nanoparticles (M=NiO, MgO, and Al_2O_3) were evaluated. Calculated optical constants for PVA-3% M (M=NiO, MgO, Al_2O_3) NPs as-prepared and after UV irradiation illustrate the impact of UV irradiation period. These data demonstrate that a highly forced for medical applications.

Received February 17, 2023; Accepted May 8, 2023)

Keywords: NiO, MgO, Al_2O_3, PVA, UV irradiation, Optical properties

1. Introduction

Due to its dielectric strength, high thermal and chemical stability, and appropriate storage capacity, as well as its optical studies, polyvinyl alcohol (PVA) has appealing usage in a variety of fields [1][2]. These types of materials are used for coating, binding industries and optoelectronic due to its significance physical investigations [3]. Due to the utilization of functional materials, doping in PVA is a crucial component of the manufacturing process [4]. It is commonly recognized that non-covalent bonds, including as hydrogen and coordination bonds, serve as the foundation for super molecular structure design [5]. The optical and electrical properties of oxides like In_2O_3, SnO_2, ZnO, CdO, In_2O, and CuO provide an intriguing feature [6][7]. The regulation of their nanoscale has an impact on these features [7]. Due to their use in transparent electrodes, solar energy conversion, gas sensing, and catalysis, materials based on metal and/or oxide have raised concerns. An appealing semiconductor with beneficial qualities for photocatalysis and chemical sensing applications is nickel oxide (NiO). It is a metal oxide that is a green chemical compound. Poinsinite is a highly rare mineral that contains nickel oxide[8]. Magnesium oxide (MgO), a white solid metal, is created when the ions of magnesium and oxygen combine. MgO is a non-conductive material with a high resistance to electric current at ambient temperature. High heat conductivity and low electrical conductivity are two of MgO's key characteristics. Magnesium carbonate or magnesium hydroxide are calcined to make it. Due to its distinct physical and chemical characteristics, magnesium oxide is very important and a promising material for usage in coatings, sensors, and catalysis [9]**.** Aluminum oxide (Al_2O_3) has two patterns, the alpha pattern

* Corresponding author: m.ahmad@ut.edu.sa
https://doi.org/10.15251/DJNB.2023.182.591

(α-Al_2O_3) and the gamma pattern(γ-Al_2O_3), which have the same chemical formula but differ from each other in the crystal structure, which makes there a difference in the physical and chemical properties[10]. On the other hand, investigations on UV irradiation[11][12][13][14] showed that UV irradiation has a significant impact on chemical composition and structure, which contributes to changes in optical characteristics. Bradford et al. observed the impact of UV irradiation on the optical characteristics of silicon oxide [14]. They explained these variations in optical characteristics by an increase in silicon oxide's oxygen molecules as a result of UV radiation exposure. Additionally, Fernández-Rodrguez et al.[12] shows that UV-irradiated TiO2 films experience two separate, distinct processes. Oxygen incorporation and surface modifications take place. When assessing the effects of ultraviolet radiation on human skin, it is important to carefully distinguish between short-wave and long-wave ultraviolet light (UV-A) (UV-B and UV-C). High levels of ultraviolet A can make the first coloration it causes permanent. This sort of ultraviolet A-induced pigmentation has been named "spontaneous" since it doesn't require an erythematous reaction to begin or speed up melanine synthesis. UVB radiation causes erythema and ensuing pigmentation. The actinic structure of the skin is harmed by prolonged exposure to ultraviolet B, which may also cause cancer. One should use the utmost caution when in the sun (global radiation). Publicity of the dangers of prolonged sun exposure is necessary. Utilizing artificial "suns" with spectra between 260 and 400 nm is not advised because they could harm the environment similarly to ambient radiation. It is strongly advised to use artificial illumination on a specific schedule. One exposure cycle must be followed by a pause before the next one may start. When artificial lamps are used regularly to tan skin, irreversible skin damage may develop. Radiation sources with emission spectra restricted to wavelengths between 315 and 400 nm are ideal for inducing skin pigmentation (cosmetic usage). Strong radiation, such as UVASUN systems, causes a "pleasant" permanent coloring after exposures lasting less than an hour [15].

In this work, there are two main objectives of these investigations: (i) to study the structural investigation of as-prepared PVA-3% M, (M=NiO, MgO, Al_2O_3) NPs and (ii) to study the change of optical properties of PVA-3% M, (M=NiO, MgO, Al_2O_3) NPs from 0 to 60 min. UV irradiation in the range UVA.

2. Experimental techniques

2.1. Preparation of metal oxides

A combustion method [16][17][18][19] was used for preparation different types of metal oxides *M=NiO, MgO* and *Al_2O_3* NPs. 25 mL water solution of 0.2 M $Ni(NO_3)_2{\cdot}6H_2O$ added to 0.2M $CO(NH_2)_2.6H_2O$ in flask. The solution was introduced into a microwave oven then operating for 20 min at a maximum power of 650 W. NiO NPs powder was extracted. The same procurer for MgO and Al_2O_3 NPs were used with $Mg(NO_3)_2{\cdot}6H_2O$ and $Al(NO_3)_2{\cdot}6H_2O$, respectively as starting material. NiO, MgO, and Al_2O_3 NP preparations were made.

2.2. Preparation of doped PVA

A PVA material with an average molecular weight of 17000 g/mol was bought from Sigma-Aldrich (see Scheme 1).

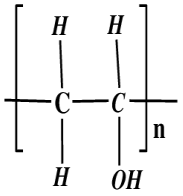

Scheme 1. The chemical structure of the PVA.

The PVA powder was soluted in water at a temperature of 353 K, and the mixture was then agitated for 30 minutes at this specific temperature. Slowly, the PVA solution's temperature was lowered to 323 K. NiO, MgO, and Al_2O_3 were mixed continuously at 323 K with 30 ml of triple-distilled water to create the suspended solution. At 323 K, the suspended solution was then mixed with the PVA solution. PVA/MgO, PVA/Al_2O_3 NPs, and PVA/NiO final mixtures are held at 323 K with constant stirring for 6 hours. The finished solution was placed in a petri plate and kept at 313 K for a few days (in our case, 8 days), allowing the solvent to evaporate. It was possible to generate a PVA sheet with a final thickness of roughly 0.08 mm.

In order to create a suspended solution with 3 wt% NiO, MgO, and Al_2O_3 doped in PVA, 3 wt% NiO, MgO, or Al_2O_3 were added to a 97 wt% PVA solution. These films are regarded as stable films if they have been stored in a desiccator under a vacuum. Additionally, it must be protected from direct sunlight to avoid the development of double bonds inside the primary chains of the PVA structure.

Ultraviolet (UV) lamp (25 W) was used for irradiation the PVA-3%M at room temperature. The distance between the lamp and PVA-3%M was kept constant during the experiment.

2.3. Characterizations

A monochromatized CuK source with a wavelength of 0.15418 nm was utilized to measure X-ray diffraction using a Shimadzu XD-3A at 4^o -25^o of 2θ. Shimadzu UV-2101) was used to measure transmittance (T) in the 190-1100 nm wavelength range at room temperature before and after UV irradiation for 60 min PVA-3%M.

3. Results and discussions

3.1. Structural investigations

Fig. 1 displays the XRD pattern of PVA and PVA that has been doped with 3 weight percent of NiO, MgO, and Al_2O_3 NPs. It has been noted that pure PVA displays a shoulder at $2\theta=22.5^o$ and a crystalline reflection at about $2\theta= 19.5^o$. These two broad peaks are PVA features and, respectively, represent reflections of (101) and (101) [20].

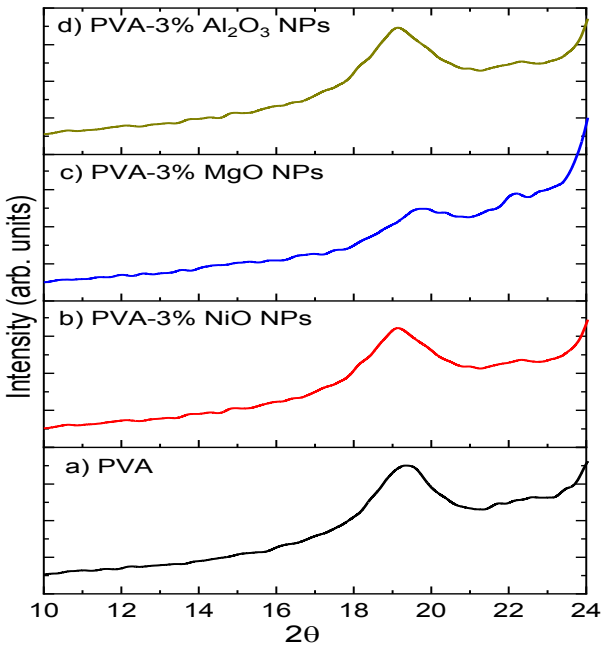

Fig. 1. XRD spectra of untreated a) PVA, b) PVA-3% NiO NPs, c) PVA-3% MgO NPs and d) PVA-3% Al_2O_3 NPs.

This shows that PVA's semicrystalline structure contains both crystalline and amorphous phases. With according to the type of doping substance, the peak at 2θ=22.5° in doped PVA has changed in both broadness and intensity. When it comes to the peak at 2θ=19.5°, as shown in Fig. 2, which shows the Gaussian curve fitting for this peak of a) PVA and b) PVA doped with 3 wt% of c) NiO NPs, d) MgO NPs, and e) Al_2O_3 NPs. Changes were made to the peaks' Full Width at Half Maximum (FWHM) values.

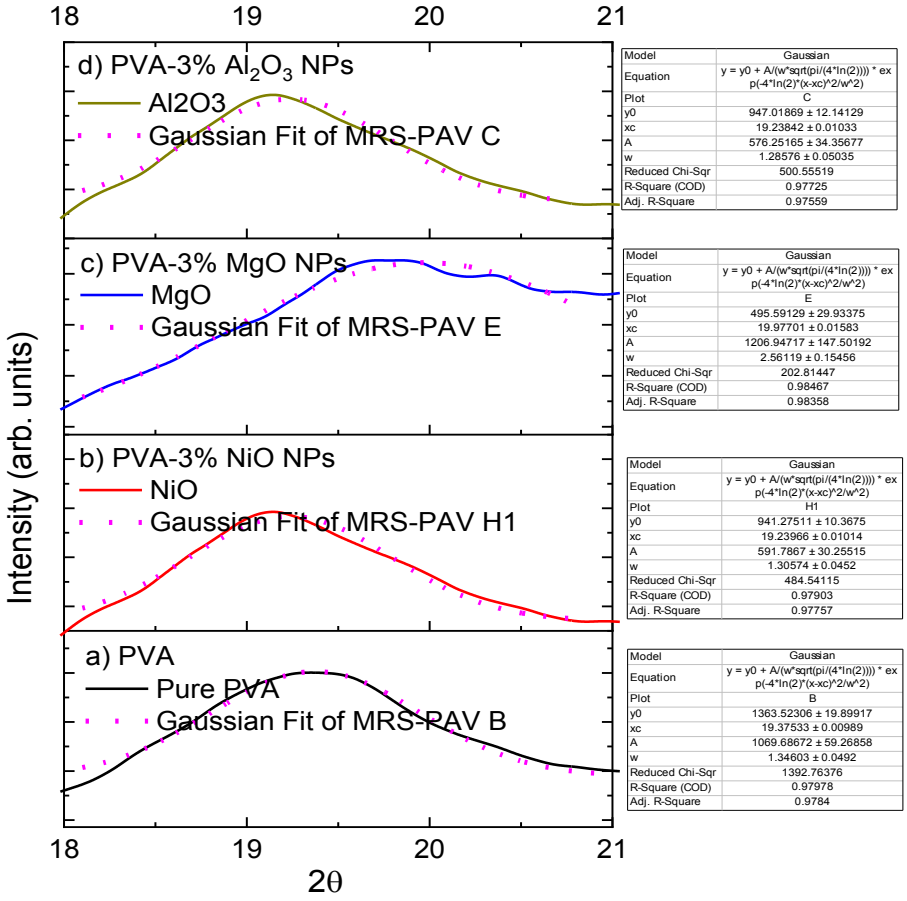

Fig. 2. Gaussian fitting curve for the mean peak of untreated a) PVA, b) PVA-3% NiO NPs, c) PVA-3% MgO NPs and d) PVA-3% Al_2O_3 NPs.

For PVA and PVA doped with 3 wt% of a) NiO NPs, b) MgO NPs, and c) Al_2O_3 NPs, the FWHM values are 1.34, 1.3, 2.5, and 1.28, respectively. As a result, the peak of PVA doped with MgO NPs is broader than that of other samples. In contrast, PVA doped with Al_2O_3 NPs had the least amount of broadness when compared to the other samples. This behavior suggests that the doped PVA samples' amorphous structure is changing [21][22]. PVA doped with 3 wt% of MgO NPs has a higher degree of amorphousness, which may be attributed to the polymer crystallizing because of less hydrogen bonds between its layers [22].

The reduction of the intermolecular hydrogen bonding between the major PVA chains may be to blame for the crystal phases breaking. Additionally, the PVA peak doped with 3 % of MgO NPs has the lowest peak intensity. The three oxygen atoms in MgO molecules may be to blame for this. Therefore, the contact between MgO NPs and the PVA structure's hydrogen bonds has a higher likelihood than the interaction between the other samples and the PVA hydrogen bond.

3.2. Studies of UV irradiation on PVA-3%M, (M=NiO, MgO, Al_2O_3) NPs

The optical absorption helps to define the band structure. Therefore, at lower frequency, its spectrum is studying the molecular vibrations. At higher frequency, its spectrum is studying atomic electronic states. The measure transmittance versus wavelength for PVA-3% M, (M=NiO,

MgO, Al_2O_3) NPs before and after UV irradiation for 60 min is represented in shown in Fig. 3. It shows an increasing behavior of transmittance after 60 min UV irradiation. The optical absorption coefficient (α) of PVA-3% M, (M=NiO, MgO, Al_2O_3) NPs before and after UV irradiation for 60 min was computed by [23].

$$\alpha = \frac{1}{d}\ln\left(\frac{1}{T}\right) \tag{1}$$

d: thickness, T: transmittance and R: reflectance.
α versus hν near the absorption edge is plotted for PVA-3% M, (M=NiO, MgO, Al_2O_3) NPs before and after UV irradiation for 60 min and shown in Fig. 4.

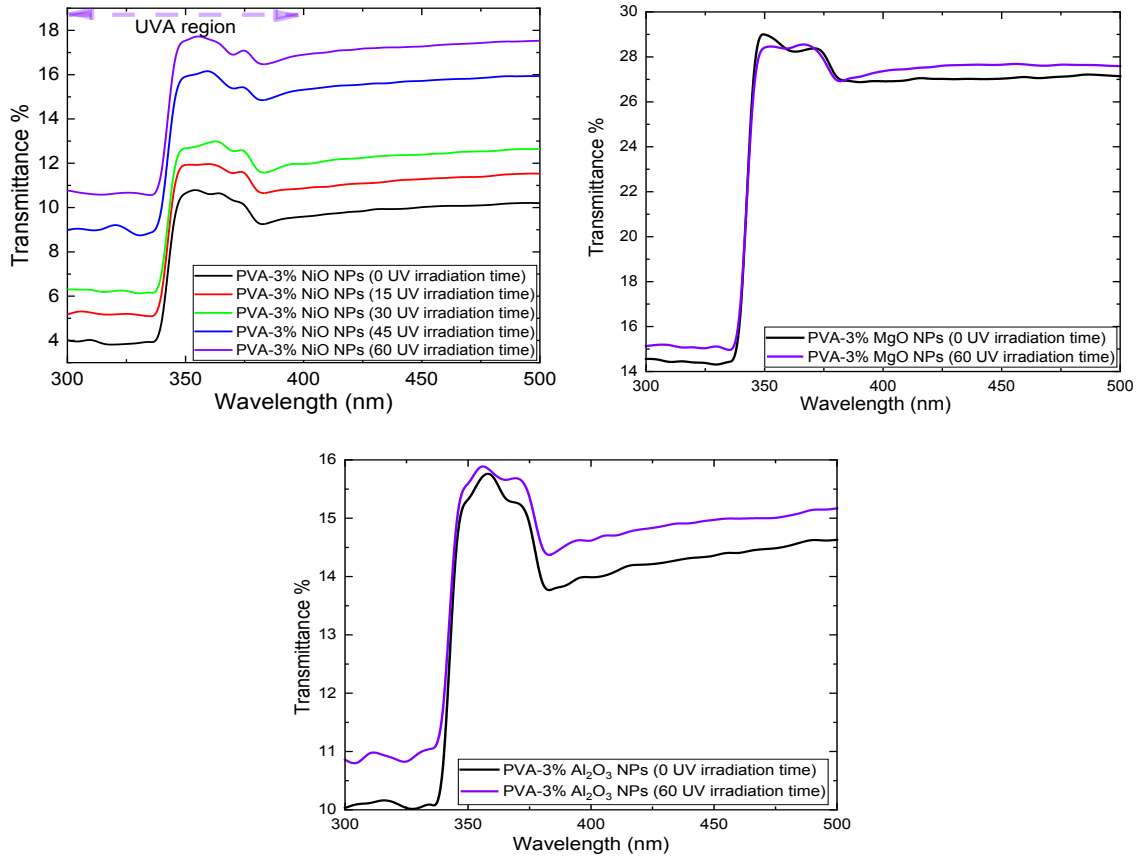

Fig. 3. Transmittance spectra of PVA-3%M, (M=NiO, MgO, Al_2O_3) nanocomposites at different time of UV irradiation.

It shows a decreasing behavior of absorption coefficient after 60 min UV irradiation. At UV irradiation time, the transmittance increases at different doped metal oxides in PVA, subsequently, the absorption coefficient decreases.

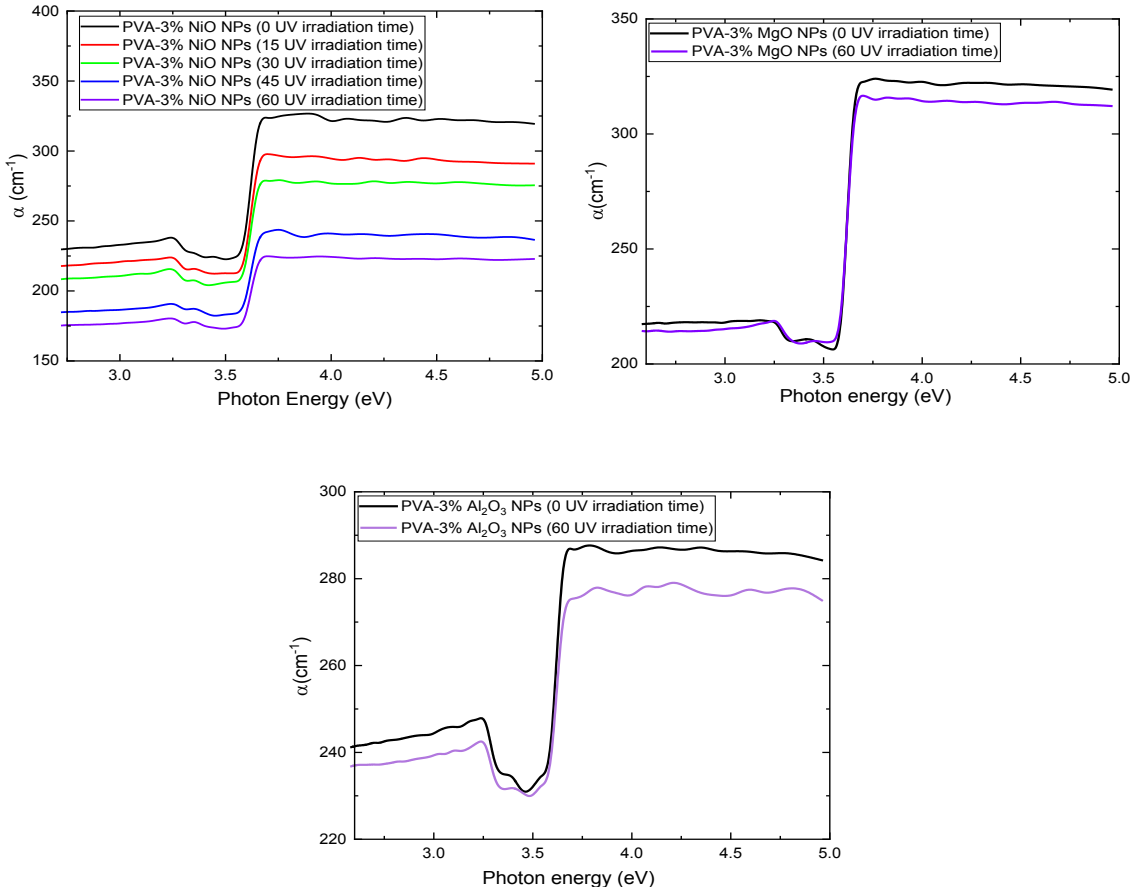

Fig. 4. Absorption coefficient (α) spectra of PVA-3%M, (M=NiO, MgO, Al_2O_3) nanocomposites at different time of UV irradiation.

As a comparison of three doped metal oxides, at zero UV irradiation time, the highest value of transmittance is for PVA/MgO, on the other hand, the lowest value of transmittance is for PVA/NiO. However, the highest value of absorption is for PVA/NiO and the lowest value is for PVA/Al_2O_3. Therefore, at lowest UV irradiation time, the PVA/NiO could be used for UV shielding. On the other hand, at 60 min. UV irradiation time, the highest value of transmittance is for PVA/MgO, on the other hand, the lowest value of transmittance is for PVA/Al_2O_3. However, the highest value of absorption is for PVA/MgO and the lowest value is for PVA/Al_2O_3. Therefore, at 60 min. UV irradiation time, the PVA/NiO could be used for UV shielding.

The equation used for calculation the value of optical gap (E_g) is [24]:

$$(\alpha h\nu)^m = C(h\nu - E_g) \quad (2)$$

C: constant, E_g: optical band gap. m: constant depends the type of the optical transition [24]. For PVA-3%M, (M=NiO, MgO, Al_2O_3) NPs before and after UV irradiation for 60 min., the value of fitting according to Eq. 2 at m=2 reflects the allowed direct transition. As a result, Fig. 5 shows the relationship between $(h\nu)^2$ and photon energy around the absorption edge for PVA-3%M, (M=NiO, MgO, and Al_2O_3) NPs before and after UV irradiation for 60 minutes.

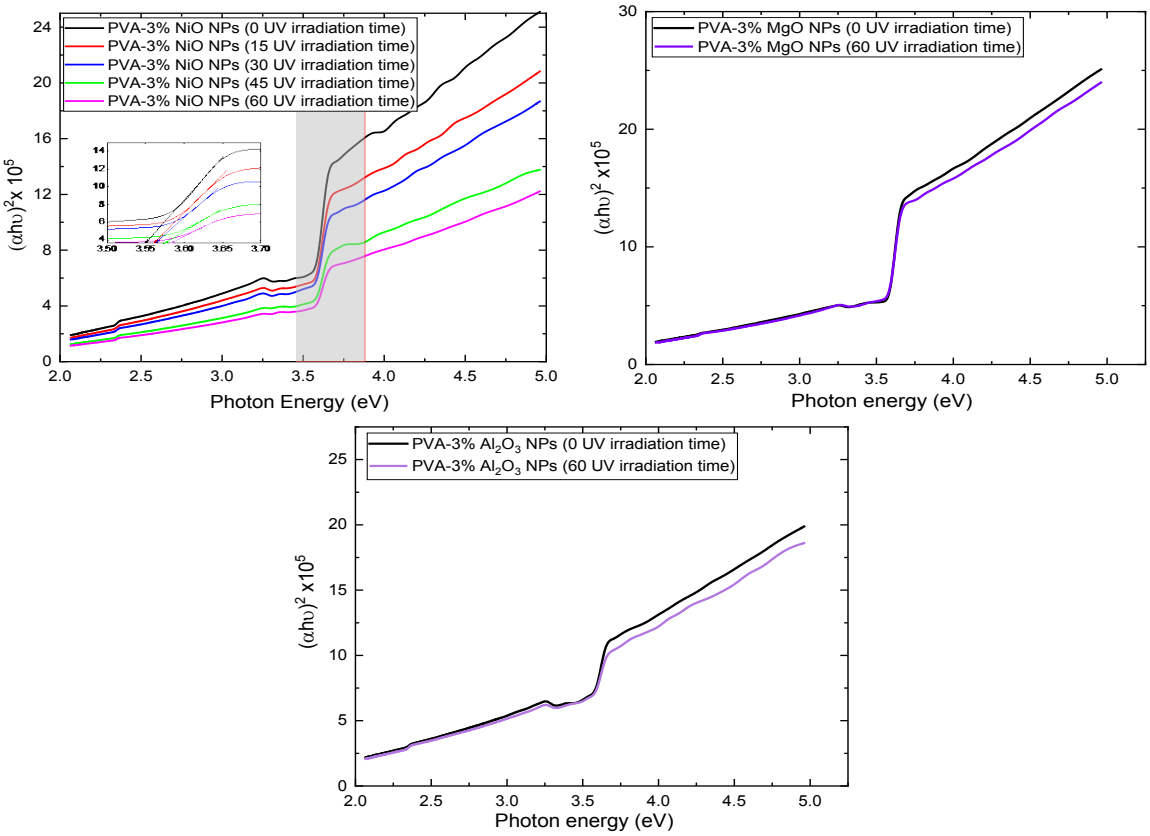

Fig. 5. $(\alpha hv)^2$ versus hv of PVA-3%M, (M=NiO, MgO, Al_2O_3) nanocomposites at different time of UV irradiation.

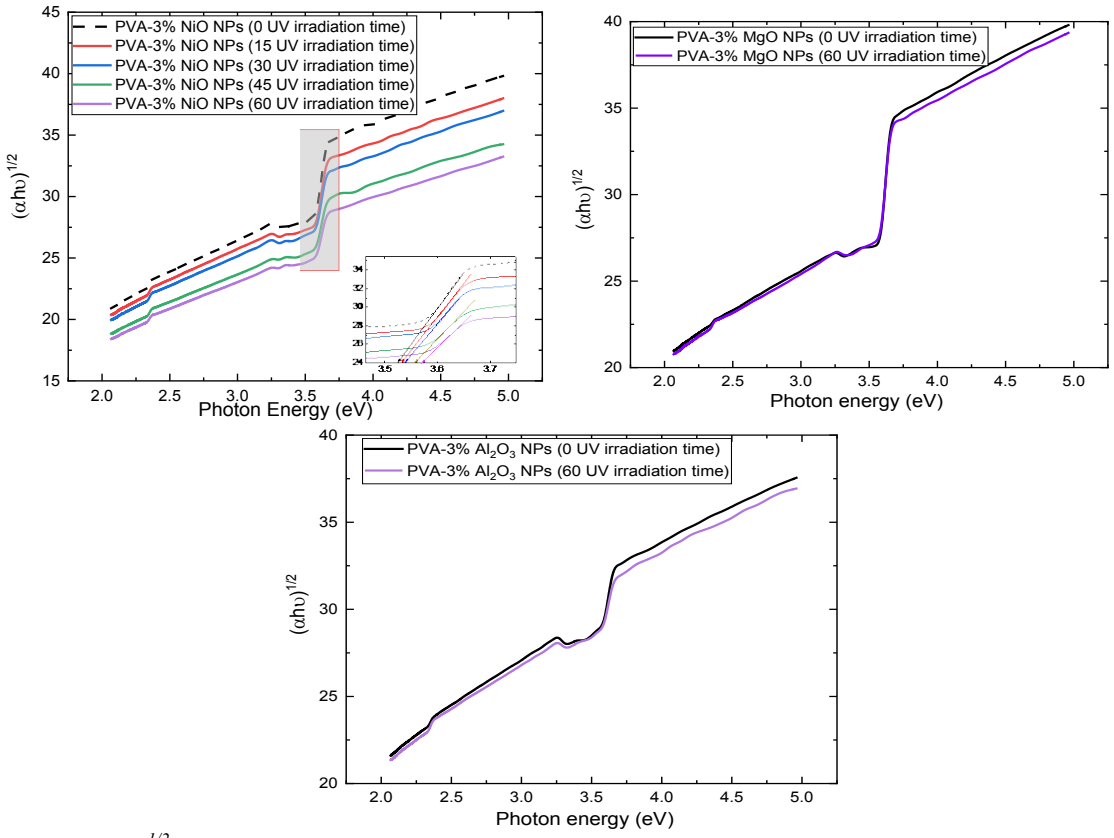

Fig. 6. $(\alpha hv)^{1/2}$ versus hv of PVA-3%M, (M=NiO, MgO, Al_2O_3) nanocomposites at different time of UV irradiation.

Moreover, the value of fitting according to Eq. 2 at m=1/2 reflects the permitted indirect transition before and after UV irradiation for 60 minutes. In Fig. 6, the $(\alpha h)^{1/2}$ versus photon energy around the absorption edge for PVA-3% M, (M=NiO, MgO, and Al_2O_3) NPs is plotted before and after UV irradiation for 60 minutes. The results of extrapolating these graphs to the hv axis to get the values of the direct and indirect optical band gap are listed in Table 1. It compares the values of the PVA-3% M, (M=NiO, MgO, and Al_2O_3) NPs before and after UV irradiation for 60 min. This shows that the un-irradiated samples have lower values.

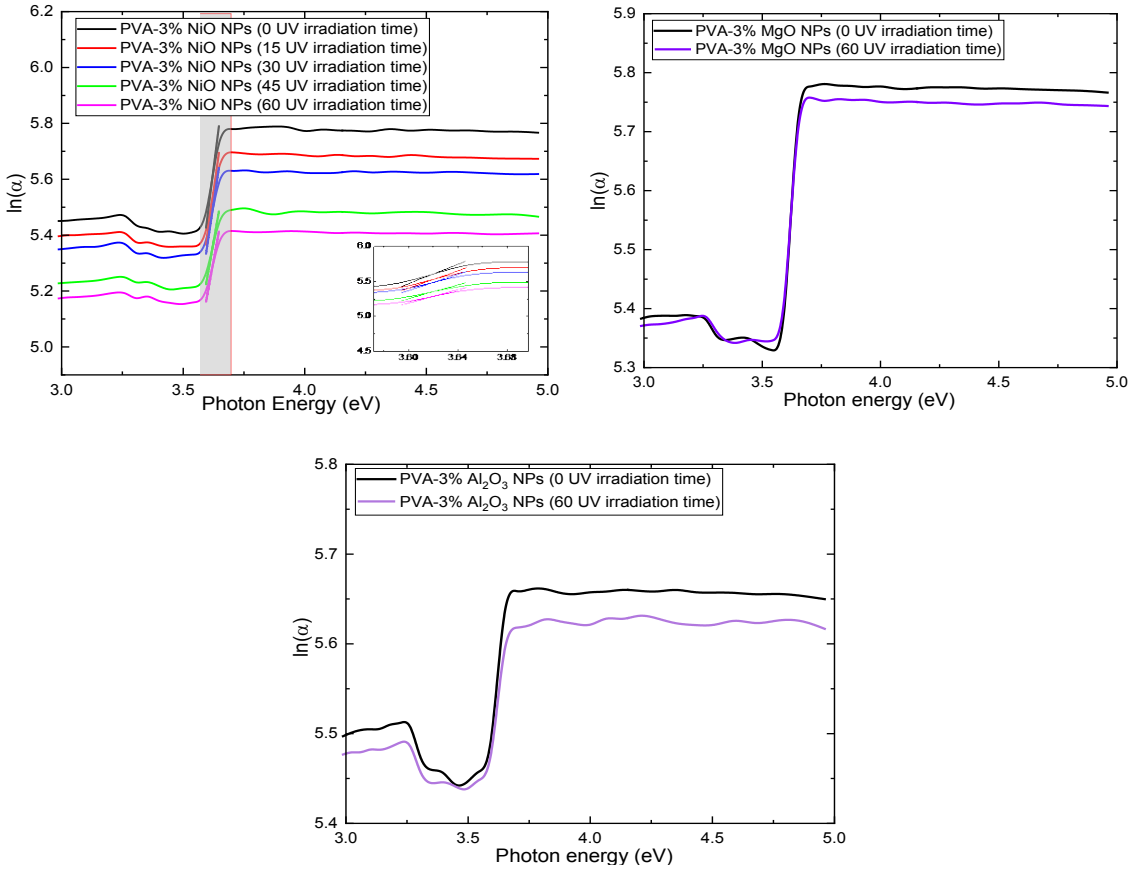

Fig. 7. ln(α) versus hv of PVA-3%M, (M=NiO, MgO, Al_2O_3) nanocomposites at different time of UV irradiation.

On the other hand, the absorption coefficient near the absorption edge complies with the empirical Urbach rule [25] at a particular temperature using this relation:

$$\alpha(\upsilon) = \alpha_0 \exp(h\upsilon / E_r) \tag{3}$$

α_0: constant, E_r: localized states width.
ln(α) vs. photon energy (hν) for PVA-3% M, (M=NiO, MgO, Al_2O_3) NPs before and after UV irradiation for 60 min is given in Fig. 7. E_r values are tabulated in Table 1.

The extinction coefficient ($k_{ext.}$) could be calculated by [25]:

$$k_{ext.} = \frac{\alpha\lambda}{4\pi} \tag{4}$$

Fig. 8 depicts the extinction coefficient ($k_{ext.}$) vs. photon energy (hv) for PVA-3% M, (M=NiO, MgO, and Al_2O_3) NPs before and after UV irradiation for 60 min. This graph shows a

decreasing tendency with both the incident photon energy and UV irradiation period. The electromagnetic wave's amplitude will decrease after crossing a thickness, and the skin depth (δ) can be computed using the following relation[26]:

$$\delta = \frac{1}{\alpha} \tag{5}$$

Fig. 9 represent the plot of skin depth versus photon energy (hν) for PVA-3% M, (M=NiO, MgO, Al_2O_3) NPs before and after UV irradiation for 60 min. From this figure, it can show that the skin depth is independent on the UV irradiation.

Table 1. Optical and dispersion parameters of PVA-3%M, (M=NiO, MgO, Al_2O_3) nanocomposites.

UV irradiation time (min.)	PVA-3% NiO			PVA-3% MgO			PVA-3% Al_2O_3		
	E_g^d (eV)	E_g^{ind} (eV)	E_e (eV)	E_g^d (eV)	E_g^{ind} (eV)	E_e (eV)	E_g^d (eV)	E_g^{ind} (eV)	E_e (eV)
0	3.55	3.52	0.147	3.576	3.57	0.30	3.54	3.55	0.67
15	3.56	3.53	0.161						
30	3.56	3.54	0.172						
45	3.57	3.56	0.200						
60	3.58	3.67	0.212	3.580	3.568	0.32	3.55	3.54	0.79

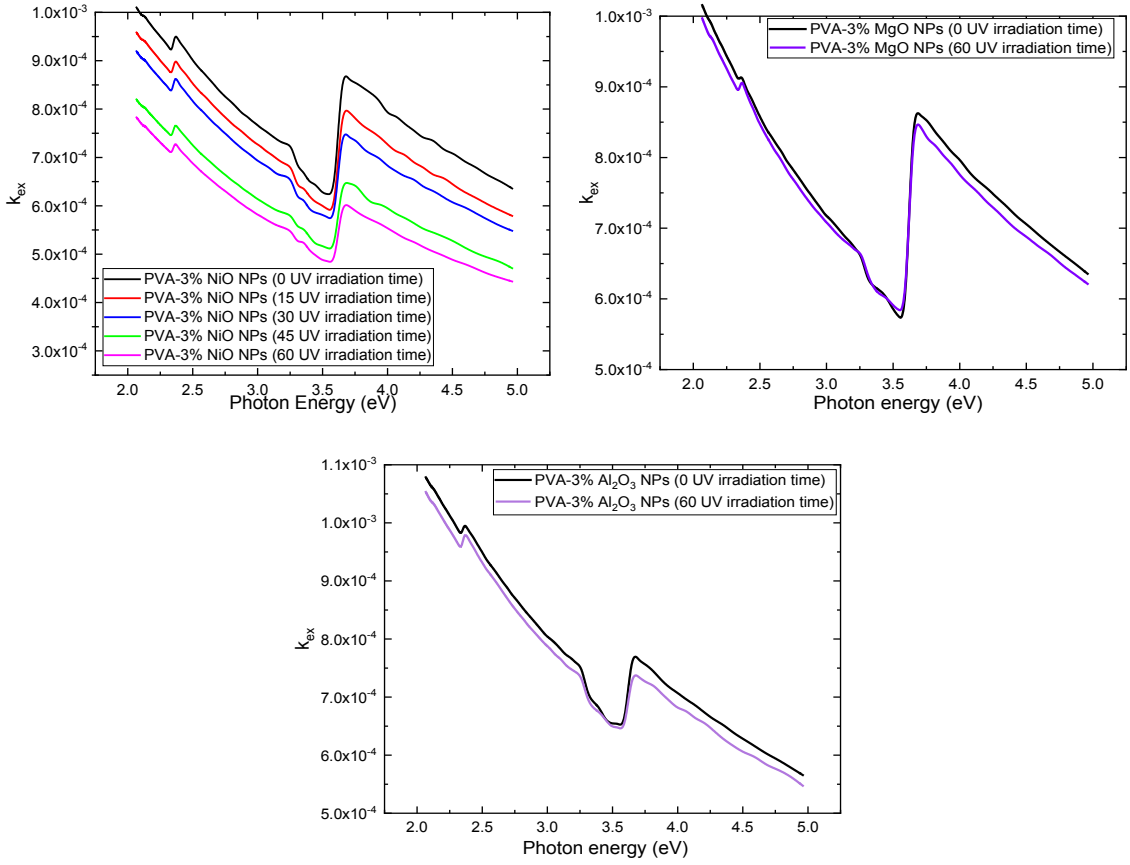

Fig. 8. Extension coefficient (k_{ex}) versus hv of PVA-3%M, (M=NiO, MgO, Al_2O_3) nanocomposites at different time of UV irradiation.

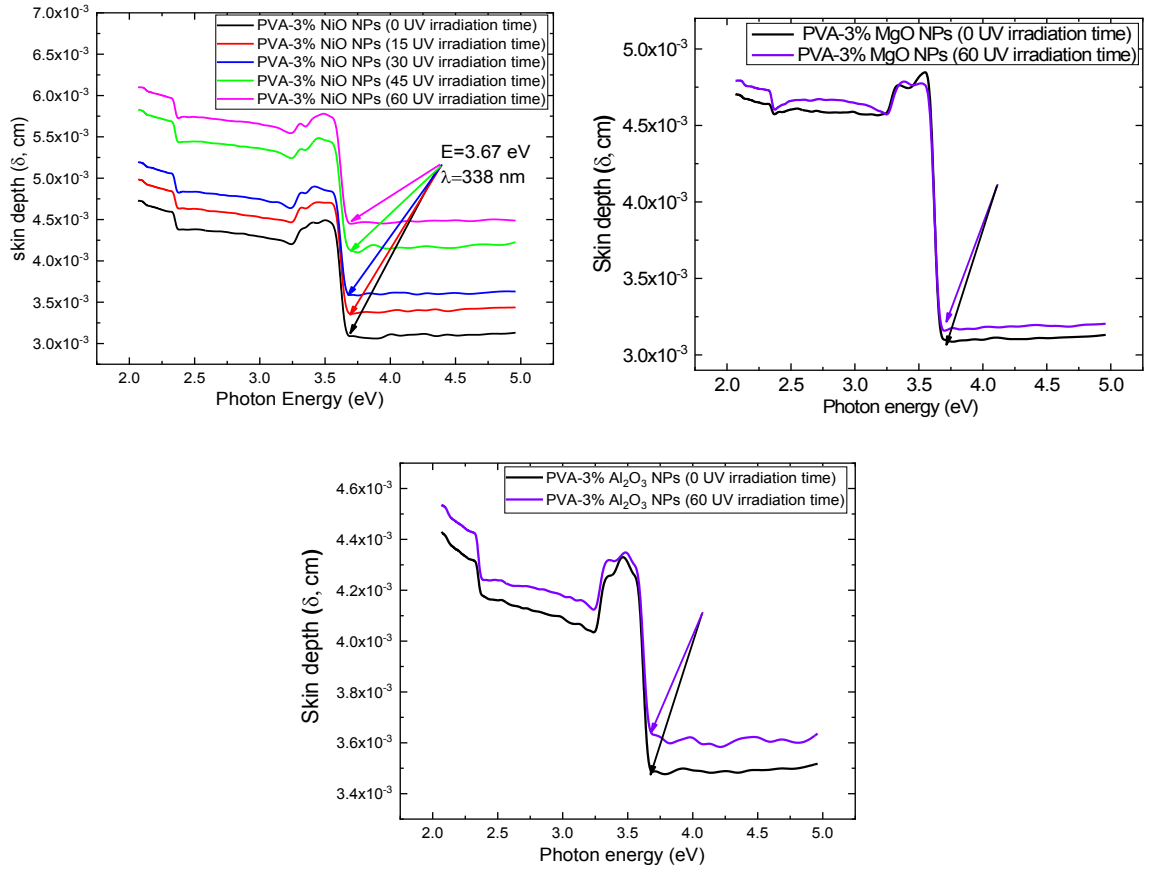

Fig. 9. Skin depth (δ) versus hv of PVA-3%M, (M=NiO, MgO, Al_2O_3) nanocomposites at different time of UV irradiation.

4. Conclusions

XRD confirms the structural characteristics of the produced PVA-3% M, (M=NiO, MgO, and Al_2O_3) NPs. The doped metal oxides affect on the optical proprties of the PVA-3% M, (M=NiO, MgO, and Al_2O_3). The synthesized PVA-3% M, (M=NiO, MgO, Al_2O_3) NPs display a modest effect of irradiation period, as indicated by a shifted absorption edge under the influence of UV irradiation. Under the influence of irradiation time, several linear optical papameters of PVA-3% M, (M=NiO, MgO, and Al_2O_3) NPs were calculated. Different doped metal oxides in PVA exhibit an increase in transmittance under UV irradiation, which causes a drop in the absorption coefficient. In a study of three doped metal oxides of PVA-3% M, (M=NiO, MgO, Al_2O_3) NPs. PVA/MgO has the maximum transmittance at zero irradiation time, However, PVA/NiO has the maximum absorption value Therefore, PVA/NiO might be employed for UV shielding at the lowest UV irradiation period. PVA/MgO exhibits the highest transmittance at 60 minutes of UV exposure; however, PVA/Al_2O_3 has the maximum absorption value. Therefore, PVA/NiO might be employed for UV shielding at the lowest UV irradiation time. Therefore, the PVA/ Al_2O_3 might be employed for UV shielding after irradiation time. It was also, illustrated that skin depth is independent of irradiation time.

References

[1] T. Tunç, Ş. Altındal, İ. Dökme, and H. Uslu, J. Electron. Mater., vol. 40, no. 2, pp. 157-164, 2011; https://doi.org/10.1007/s11664-010-1440-9

[2] M. Diallo et al., J. Chem. Crystallogr., vol. 38, no. 6, pp. 475-478, 2008;

https://doi.org/10.1007/s10870-008-9349-3

[3] L. L. Beecroft and C. K. Ober, Chem. Mater., vol. 9, no. 6, pp. 1302-1317, 1997; https://doi.org/10.1021/cm960441a

[4] D. Singh, S. Kumar, and R. Thangaraj, Phase Transitions, vol. 87, no. 2, pp. 206-222, 2014; https://doi.org/10.1080/01411594.2013.788181

[5] K. P. Mörtl, J.-P. Sutter, S. Golhen, L. Ouahab, and O. Kahn, Inorg. Chem., vol. 39, no. 8, pp. 1626-1627, 2000; https://doi.org/10.1021/ic9911825

[6] J. X. Wang et al., J. Cryst. Growth, vol. 267, no. 1-2, pp. 177-183, 2004; https://doi.org/10.1016/j.jcrysgro.2004.03.052

[7] D. Zhang, L. Sun, J. Yin, and C. Yan, Adv. Mater., vol. 15, no. 12, pp. 1022-1025, 2003; https://doi.org/10.1002/adma.200304899

[8] M. El-Kemary, N. Nagy, and I. El-Mehasseb, Mater. Sci. Semicond. Process., vol. 16, no. 6, pp. 1747-1752, 2013; https://doi.org/10.1016/j.mssp.2013.05.018

[9] R. Wahab, S. G. Ansari, M. A. Dar, Y. S. Kim, and H. S. Shin, Materials Science Forum, 2007, vol. 558, pp. 983-986; https://doi.org/10.4028/www.scientific.net/MSF.558-559.983

[10] A. Z. Ziva, Y. K. Suryana, Y. S. Kurniadianti, A. B. D. Nandiyanto, and T. Kurniawan, Mech. Eng. Soc. Ind., vol. 1, no. 2, pp. 54-77, 2021; https://doi.org/10.31603/mesi.5493

[11] M. Purica et al., Thin Solid Films, vol. 515, no. 24, pp. 8674-8678, 2007; https://doi.org/10.1016/j.tsf.2007.03.117

[12] M. Fernández-Rodríguez, V. J. Rico, A. R. González-Elipe, and A. Álvarez-Herrero, Phys. status solidi c, vol. 5, no. 5, pp. 1164-1167, 2008; https://doi.org/10.1002/pssc.200777790

[13] A. H. Moharram, S. A. Mansour, F. Al-Marzouki, A. A. Hendi, and M. Rashad, Mater. Sci. Pol., vol. 31, no. 1, pp. 139-145, 2013; https://doi.org/10.2478/s13536-012-0080-6

[14] A. P. Bradford and G. Hass, JOSA, vol. 53, no. 9, pp. 1096-1100, 1963; https://doi.org/10.1364/JOSA.53.001096

[15] W. Raab, Z. Hautkr., vol. 55, no. 8, pp. 497-513, Apr. 1980.

[16] M. Rashad, N. M. Shaalan, and A. M. Abd-Elnaiem, Desalin. Water Treat., vol. 57, no. 54, pp. 26267-26273, 2016; https://doi.org/10.1080/19443994.2016.1163511

[17] M. Rashad, M. Rüsing, G. Berth, K. Lischka, and A. Pawlis, J. Nanomater., vol. 2013, p. 82, 2013; https://doi.org/10.1155/2013/714853

[18] N. M. Shaalan, M. Rashad, and M. A. Abdel-Rahim, Opt Quant Electron, vol. 48, p. 531, 2016; https://doi.org/10.1007/s11082-016-0802-9

[19] A. M. Abd-Elnaiem, T. A. Hamdalla, S. M. Seleim, T. A. Hanafy, M. Aljohani, and M. Rashad, J. Inorg. Organomet. Polym. Mater., vol. 31, no. 10, pp. 4141-4149, 2021; https://doi.org/10.1007/s10904-021-02035-9

[20] R. Ricciardi, F. Auriemma, C. De Rosa, and F. Lauprêtre, Macromolecules, vol. 37, no. 5, pp. 1921-1927, 2004; https://doi.org/10.1021/ma035663q

[21] C. U. Devi, A. K. Sharma, and V. V. R. N. Rao, Mater. Lett., vol. 56, no. 3, pp. 167-174, 2002; https://doi.org/10.1016/S0167-577X(02)00434-2

[22] A. Hassen, T. Hanafy, S. El-Sayed, and A. Himanshu, J. Appl. Phys., vol. 110, no. 11, p. 114119, 2011; https://doi.org/10.1063/1.3669396

[23] A. A. A. Darwish, M. Rashad, A. E. Bekheet, and M. M. El-Nahass, J. Alloys Compd., vol. 709, pp. 640-645, 2017; https://doi.org/10.1016/j.jallcom.2016.08.280

[24] M. Rashad, Opt. Mater. (Amst)., vol. 105, no. March, p. 109857, 2020; https://doi.org/10.1016/j.optmat.2020.109857

[25] A. A. El-Fadl, G. A. Mohamad, A. B. A. El-Moiz, and M. Rashad, Phys. B Condens. Matter, vol. 366, no. 1-4, pp. 44-54, 2005; https://doi.org/10.1016/j.physb.2005.05.019

[26] T. Toyoda, J. Phys. D. Appl. Phys., vol. 18, no. 8, pp. L129-L134, Aug. 1985; https://doi.org/10.1088/0022-3727/18/8/008